

# Impact Analysis of Ultra High Performance Fiber Reinforced Concrete using Finite Element Analysis

**Prabhash Kumar**

M.Tech Student, Department of Civil Engineering, Roorkee Institute of Technology, Roorkee, Haridwar, UK-247667

**Dr. Amrendra Kumar**

Department of Civil Engineering, Roorkee Institute of Technology, Roorkee, Haridwar, UK-247667

## ABSTRACT

With the advancement in technology, UHPFRC is invented which includes exceptionally high mechanical properties (stress, strain, toughness and energy absorption capacity) and durability properties (permeability, creep, fatigue and corrosion resistance). Therefore, it attracts the researchers to investigate it in depth. Due to the difficulty in performing the impact test over UHPFRC, finite element study is made with the help of a commercially available FEM software ANSYS. An attempt has been made to verify the finite element results with the experimental results obtained in the laboratory and then obtain various other critical parameters (toughness, energy absorption capacity, failure pattern, crack propagation) through ANSYS only. There is not any recommended procedure or standard code available to perform the impact test over concrete, because of which every other researcher have used different shape, size, and geometry of fiber and concrete specimen which result in variability of results obtained through experiments. Therefore, the model is drawn in “ANSYS workbench” and other properties are assigned in “ANSYS mechanical” along with the assignment of “8 noded SOLID65” element, and “Hydrodynamic code” solver from LS-DYNA is used for obtaining the post processing results instead of the default “ANSYS AUTODYN” solver in ANSYS.

**KEYWORDS:** ANSYS, Toughness, Energy Absorption Capacity, Failure Pattern, Crack Propagation.

## I. INTRODUCTION

This One of the high strength concretes developed in the final ten years of the 20<sup>th</sup> century is ultra-high-performance concrete. It is characterized by cement weight higher than 600Kg, fine aggregate size less than 6mm, pozzolanas and the water/cement ratio less than 0.2 per cubic meter volume **Buttignol et.al. (2017)**. The mixture of above constituents in correct proportion leads in a dense and low interconnected pores with compressive strength higher than 150MPa.

With the advancement of technology, researchers added fibre in UHPC to arrest the crack propagation in the concrete arising specially during the impact loads. It results in better properties than UHPC, including increased toughness, tensile and compressive strength, and other characteristics. The resultant concrete was known as UHPFRC. Better durability qualities like low permeability, low creep strain, and a longerservice life are features of UHPFRC.

The primary problem in concrete is its brittle failure and strain softening behavior. The strain softening behavior in concrete is observed due to pull out resistance of fiber which leads to the stable propagation of crack. The fiber bridging effect in UHPFRC makes it suitable for higher load applications without

loss of considerable strength. Fiber bridging results in lesser crack width, hence UHPFRC helps in fulfilling the “Limit state of serviceability” criteria Buttignol et.al. (2017).

**OBJECTIVE**

- To study the effect of pozzolanas in UHPFRC
- Study the experimental investigation of UHPFRC under impact loading
- To determine the dynamic properties of UHPFRC through drop impact test.
- Modelling of UHPFRC and validation with experimental results
- Determination of dynamic increase factor and capacity increase factor

**II. TEST AND METHOD**

*A. Effect of Pozzolanas in FRC*

Pozzolan are the materials siliceous or siliceous aluminous material which do not have any binding property. But these materials chemical react with the calcium hydroxide at ordinary temperature which induces the binding property in these materials which mixed in finely divided form. The pozzolanas are divided in to two categories based on their availability.

The compressive strength of plain concrete increased by 21% when silica fume was added, while polypropylene fiber reinforced concrete saw a 23% increase. The strength of the concrete did somewhat decrease with the addition of fly ash or slag, but no other significant changes were observed. In accordance with ASTM C39-14, cylindrical specimens measuring 152 x 305 mm were used for the compressive strength test.

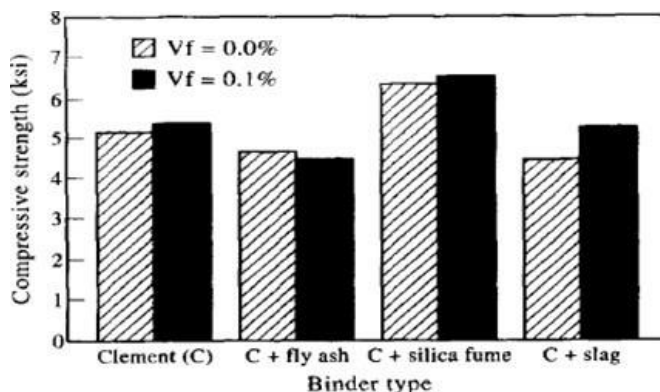


Fig 1a: Impact of fiber volume percentage and pozzolanic materials on compressive strength

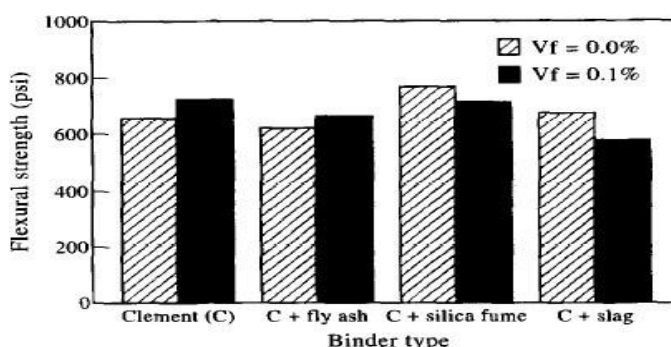


Fig 1b: Effects of pozzolanic materials and fibre volume fraction on flexural strength

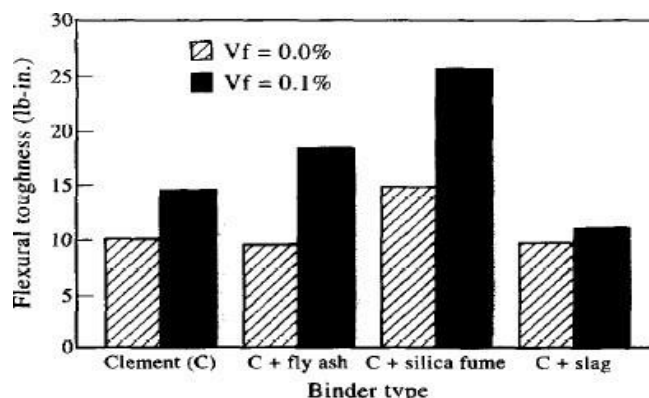


Fig 1c: Effects of pozzolanic materials and fibre volume fraction on flexural toughness

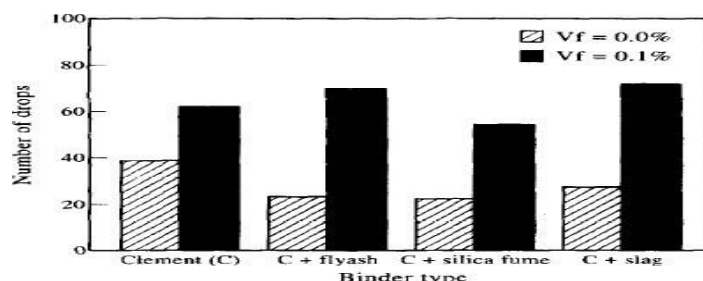


Fig. 1d: Effects of pozzolanic materials and fibre volume fraction on failure impact resistance

The compressive strength of plain concrete increased by 21% when silica fume was added. While polypropylene fiber reinforced concrete saw a 23% increase. The strength of the concrete did somewhat decrease with the addition of fly ash or slag, but no other significant changes were observed. In accordance with ASTM C39-14, cylindrical specimens measuring 152 x 305 mm were used for the compressive strength test.

The flexural strength of plain and polypropylene fiber reinforced concrete did not differ significantly since the matrix phase primarily controls the first crack strength. As per ASTM C78, the flexural strength tests are carried out.

The fibers in concrete are introduced to increase the toughness of concrete. The same can be observed from fig 1c. Due to weak bonding between polypropylene fibers and plain concrete containing slag and fly ash, there was no significant difference in flexural toughness was observed. But the addition of fibers in all the cases increased the flexural toughness in the range of 20-68%. Also the addition of silica fume in plain concrete also increase the flexural toughness because of its high reactivity and forming dense matrix. The flexural toughness test is carried according to ASTM C1018.

After that, impact loading is applied to the same concrete. However, because pozzolanas are not as reactive as cement, adding them to plain concrete decreases its impact resistance; adding fibers, however, increases impact resistance. In fig 3.1d, the comparative outcomes are displayed.

With the addition of fly ash, slag, and silica fume, respectively, the first crack strength increased by 150%, 77%, and 90%, and the failure impact resistance increased by 202%, 145%, and 164% with the addition of pozzolanas.

B. Effect of Pozzolan (silica fume) in steel fiber-reinforced concrete

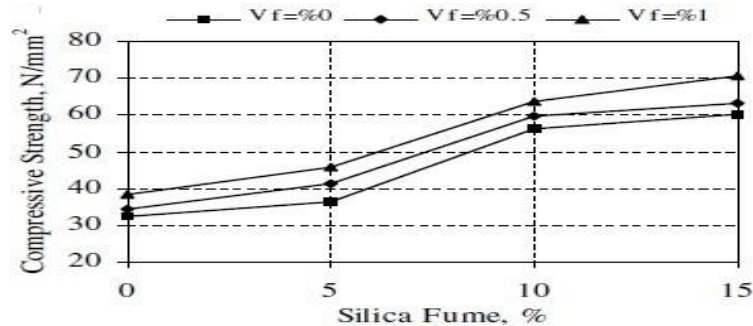


Fig 2a: The relations between compressive strength and silica fume content

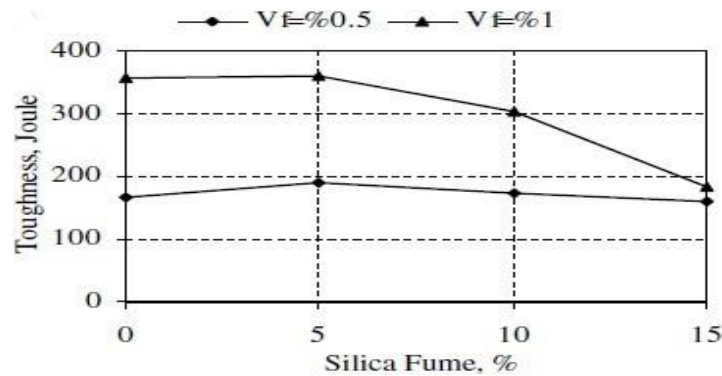


Fig 2b: The relations between flexural strength and silica fume content

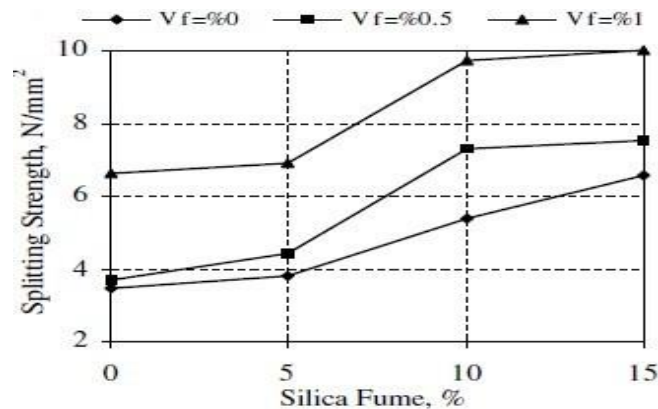


Fig 2c: The relations between toughness strength and silica fume content

As per ASTM C1018, a beam specimen measuring 150 x 150 x 500 mm is used for the flexure test. Due to its extremely fine grinding, silica fume gives concrete more density and fortifies the connection between the matrix phase and the fiber. Consequently, it fosters fiber bridging following matrix phase cracking and raises the fiber-reinforced concrete's ultimate tensile strength, flexural strength, and toughness. The robustness of steel fiber reinforced concrete remained largely unchanged with the addition of silica fume. However, the toughness showed a decrease as the silica fume content in the fiber reinforced concrete increased, particularly within the 0% to 5% range. The presence of silica fume seems to influence the fracture behavior of the fibers by enhancing the pull-out stress capacity and reinforcing the bond between the fibers.

C. Effect of Pozzolan (silica fume) in basalt fiber-reinforced concrete

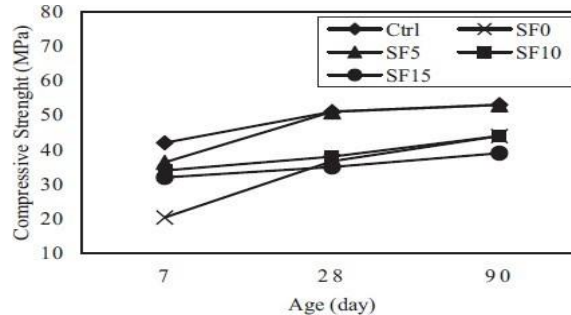


Fig 3: Effect of silica fume on compressive strength basalt fibre (1%) on cementitious composite

ASTM C109 defines the procedure for conducting the flexure strength test, and ASTM C348 gives the procedure for determining the compressive strength of concrete. In the case under consideration Prism geometry is used for determining the flexural strength and concrete cube to determine the compressive strength.

The compressive strength of plain concrete was enhanced by the addition of silica fume; however, the compaction property of concrete is decreased and compressive strength is decreased upon the addition of basalt fibers.

Although the addition of basalt fibers to concrete decreased its compressive strength, the longitudinal arrangement of the fibers stopped the spread of tensile cracks, resulting in increases in flexural strength of 12%, 31%, and 39% for concrete containing 1% basalt fiber and 5%, 24%, and 47% for reinforced concrete containing 1.5% basalt fiber.

However the flexure strength of plain concrete also increased by 5%, 10%, and 15%.

D. Effect of Pozzolan (rice husk) in macro synthetic fiber-reinforced concrete

- When rice husk ash is added to concrete instead of cement, the binding property of the concrete is increased, but the strength of the concrete begins to decline. when the content of rice husk ash increased beyond 4% in 0.15% fibre reinforced concrete.
- The addition of rice husk ash strengthen the matrix phase of concrete and improves the bonding with fibres, which ultimately improve the toughness of FRC.

E. Drying shrinkage of concrete

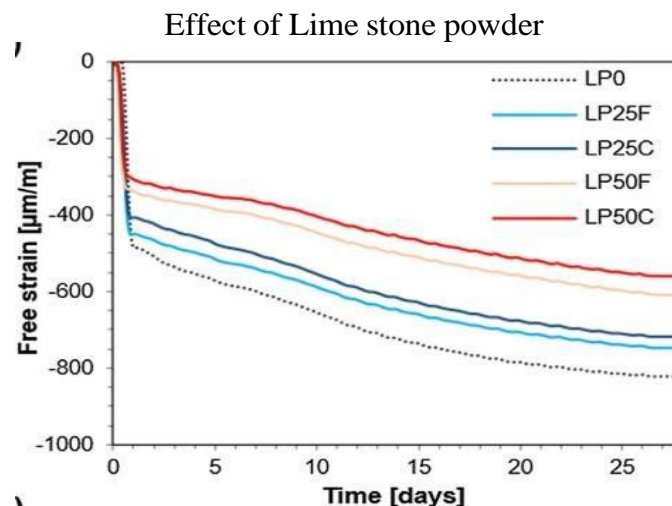


Fig 4: Autogenous shrinkage of concrete

ASTM C157 defines the procedure for determine the shrinkage of concrete. In the case under consideration, the shrinkage test was performed over prism specimen. The addition of lime stone reduce the shrinkage of concrete by 9%-32% when 25%-50% cement was replaced by lime stone powder

F. Effect of Fly ash

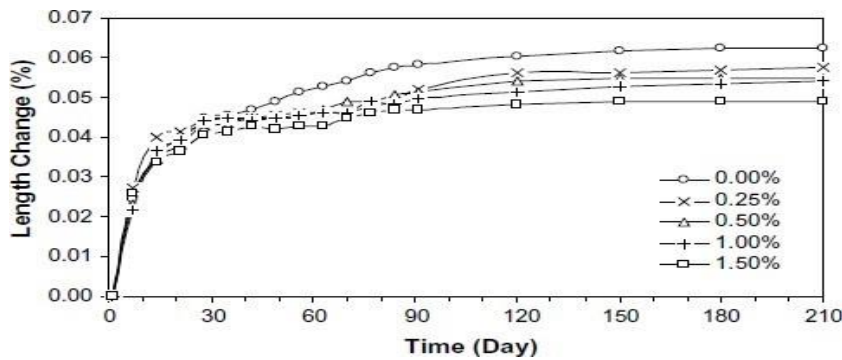


Fig 5a: Shrinkage 15% fly ash fibre reinforced concrete vs. time

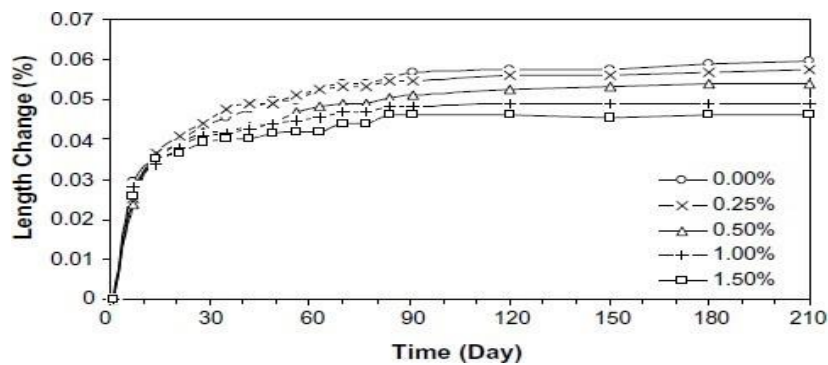


Fig 5b: Shrinkage 30% fly ash fibre reinforced concrete vs. time

When 15% fly ash was added to steel fiber reinforced concrete, concrete shrinkage was reduced by 8%, 12%, 13%, and 24%; in plain concrete, shrinkage was reduced by 4%, 9%, 18%, and 22% when 30% fly ash was added. Effect of Silica fume and metakaolin.

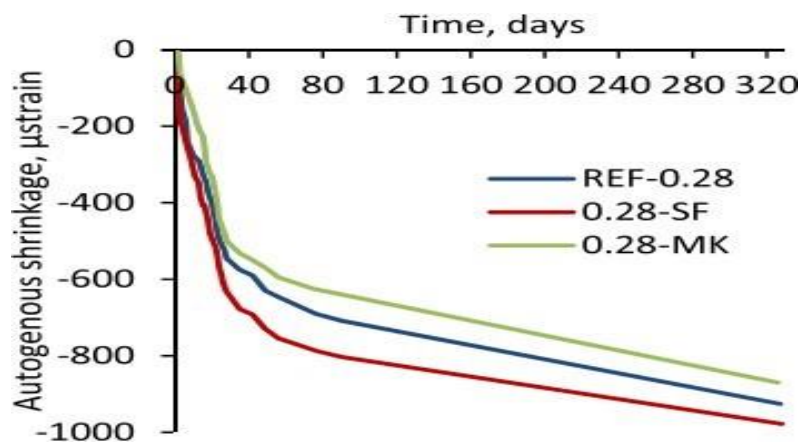


Fig 6a: Autogenously shrinkage v/s time

- The introduction of silica fume in concrete had negative impact over the Autogenous shrinkage. Instead of reducing the shrinkage the silica fume increased the shrinkage of concrete when the test performed with w/b ratio of 0.28 and 0.35

- Although the use of metakaolin reduced the Autogenous shrinkage of concrete significantly at the w/b ratio of 0.28 but there was no significant improvement in Shrinkage when the experiment was performed with the w/b ratio of 0.35

### III. MIX PROPORTIONING OF UHPFRC

UHPFRC is a kind of mixture of UHPC and FRC, including the best properties of both the concretes. It includes highstrength fibers and very high strength matrix phase, and both of them simultaneously govern the ultimate strength of UHPFRC.

Since it is primarily manufactured in industries under higher supervision therefore the chances of failure of fibers in dispersed phase are very less. In revert of that, the concrete is manufactured by unskilled labour at site and hence care should be taken while mix proportioning of UHPC or UHPFRC because in these cases the concrete also needs to withstand very high loads.

#### A. Cement content in UHPFRC

UHPFRC is characterized by high amount of cement in the mixture inducing better binding properties to hold other ingredients together. But increasing the magnitude of cement or increasing the fineness of cement in the mixture demands for more water which is not possible to be added in UHPFRC. Therefore it is like the compromising one property for the other. Researchers have been investigated high amount of cement in manufacturing of UHPFRC. Rossi utilized 1000 Kg/m<sup>3</sup> of binder while Rossi (2012) utilized 1050 Kg/m<sup>3</sup> of cement in mix proportioning of UHPFRC.

Since the cost of cement is major factor in avoiding the UHPFRC, therefore the researchers investigated the influence of pozzolanas in UHPFRC. El-Dieb et al. (2009) utilized the cement content of 900 Kg/m<sup>3</sup> along with 135 Kg/m<sup>3</sup> of silica fume. Hassan et al. (2012) reduced the cement content up to 600 Kg/m<sup>3</sup> and replaced the cement with GGBS and silica fume. Although the strength of concrete reduced with the replacement of cement content, but the reduction was under 10% of compressive strength when obtained without pozzolanas. The researchers suggest not to replace too much of cement with limestone powder and fine quartz because results in reduction of strength. Since water is required for complete hydration of cement but it reduces the strength of concrete and hence finding the relationship between optimum water content and cement content is still a challenge for the investigators. Although 'De Larrard and Sedran (1994) proposed the concept of virtual density to establish the above relationship. Virtual density is the ratio of actual concrete produced at the site and the concrete containing only solid particles without any voids.

### IV. RESULTS AND DISCUSSION

Some of the test results obtained through research papers are given here. The fibers are primarily introduced in concrete to increase the ductility, post cracking behavior toughness of the concrete. The quasi-static strength are needed to represent the results of impact resistance capacity, so some of the results static compressive and tensile strength results are also presented in this chapter. At the last of this chapter, CIF and DIF graphs are also presented to see how the dynamic increase factor vary with the rate of loading.

Table 1 Constituents of UHPFRC Spiesz, and Brouwers (2014)

Materials	UHPC1 (kg/m <sup>3</sup> )	UHPC2 (kg/m <sup>3</sup> )	UHPC3 (kg/m <sup>3</sup> )
CEM I 52.5 R	874.9	612.4	699.9
Limestone	0	262.5	0
Quartz	0	0	175.0
Microsand	218.7	218.7	218.7
Sand 0-2	1054.7	1054.7	1054.7
Micro-silica	43.7	43.7	43.7
Water	202.1	202.1	202.1
Superplasticiser	45.9	45.9	45.9
Water/cement ratio	0.23	0.33	0.29

UHPFRC is primarily employed in case of high strength concrete where ductility is needed such as in case of structures subjected to impact loads. The addition of fibers primarily increases the tensile and flexural strengths, but it also affects the compressive strength. The cement and pozzolanic contents of UHPC or UHPFRC primarily determine its compressive strength when all other factors stay constant. The addition of pozzolanas causes the concrete's compressive strength to drop.

Table 2 Comparison of binder amount and comp strength of UHPFRC at 28 days Spiesz, and Brouwers (2014)

SampleID	Cement 3(Kg/m )	GGBS 3(Kg/m )	SF 3(Kg/m )	w/b Ratio	Steeffiber (Vol %)	Compressive strength at 28 days(MPa)
UHPC 1	869	0	43	0.18	2.4	155
UHPC 2	599	0	43	0.18	2.4	139
UHPC 3	699	0	43	0.18	2.4	150

In the above cases UHPC1 is the control mixture with the cement content of 874.9 Kg/m<sup>3</sup>. 262.5 Kg/m<sup>3</sup> cement is replaced by limestone with reduction in compressive strength of 9%, and 175 Kg/m<sup>3</sup> cement is replaced by quartz with reduce in compressive strength of 4.5%. Hence it can be observed that keeping the other factors constant, the cement content can be replaced with suitable pozzolanas to approach the economy because the less w/b ratio in UHPFRC reduces the hydrated cement content and it needs to be replaced with pozzolanas.



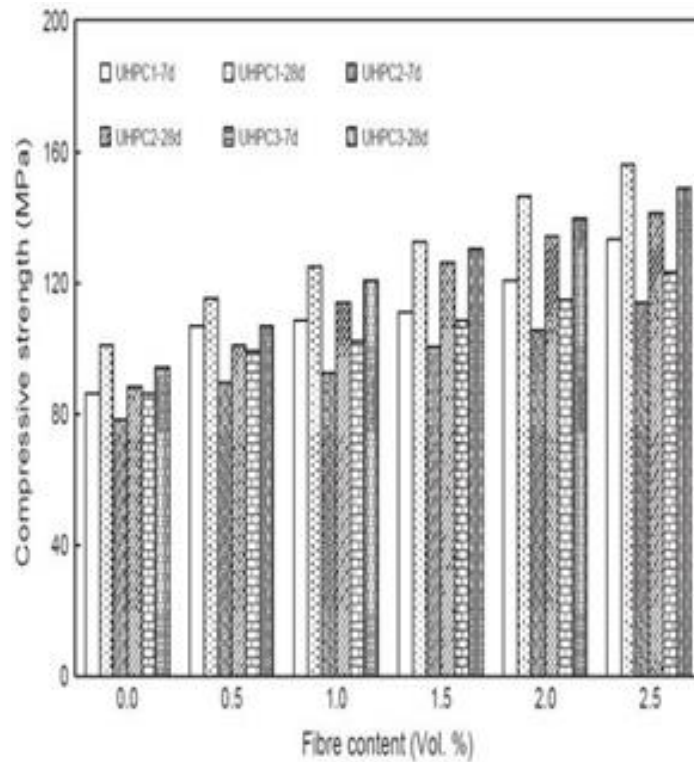


FIG 7A FLEXURAL STRENGTH OF UHPFRC AFTER 7 AND 28 DAYS Spiesz, and Brouwers (2014)

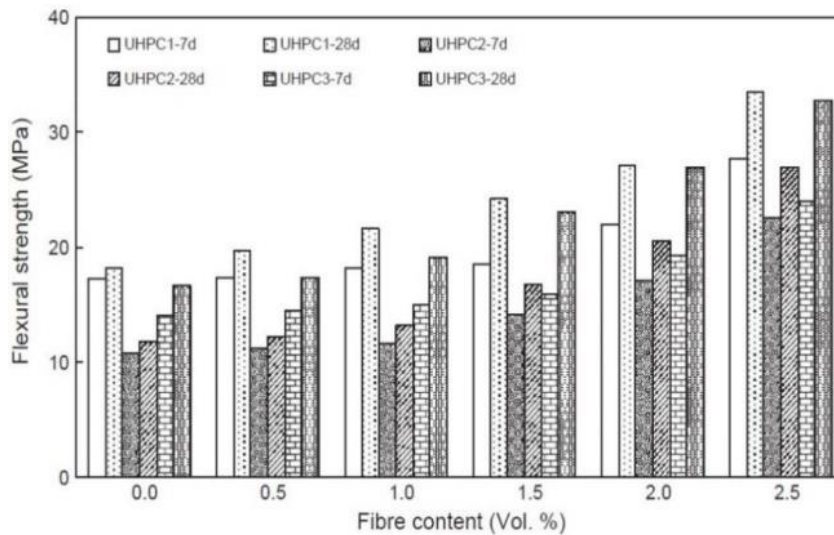


Fig 7b Compressive strength of UHPFRC after 7 and 28days Spiesz, and Brouwers (2014)

As the fiber content increases, so do the flexural and compressive strengths. When 2.5% steel fibers are added, however, the increases in compressive strength are 58%, 55%, and 56%, respectively, after 28 days. When 2.5% steel fibers are added, the flexural strength increases by 89%, 117%, and 106%, respectively, after 28 days.

Table 3 Composition UHPFRC (Habel and Gauvreau 2008)

Constituent	Type	Weight (kg/m <sup>3</sup> )
Cement	Portland cement	967
Silica fume	White, specific surface: 15-18 m <sup>2</sup> /g	251
Silica sand	Size < 0.5 mm	675
Steel fibers	Straight (length/diameter: 10 mm/0.2 mm)	430
Superplasticizer	Polycarboxylate	35
Total water		244

Table 4 Constituents of UHPFRC (Popaet al. 2013)

Constituents	No fibers		With fibers	
	M1	M2	M3	M4
Cement	1	1	1	1
w/b ratio	0.26	0.26	0.28	0.26
Super plasticizer	0.05	0.05	0.04	0.05
Silica fume	0.28	0.24	0.28	0.24
Quartz powder	0.69	0.64	0.69	0.64
Fiber	0	0	0.12	0.21
Sand	0.53	0.49	0.53	0.51
Andesite	0.89	0.84	0.93	0.84

\*mix proportions by weight of cement

Table 5 Properties of UHPFRC (Popaet al. 2013)

Strength	Age (Days)	No fibers		With fibers	
		M1	M2	M3	M4
f <sub>cm</sub>	1	65.1	86.9	86.6	90.1
	7	88.7	110.9	115.4	120.1
	28	91.7	138.6	145.7	160.4
f <sub>ctm</sub>	28	6.9	8.8	14.9	15.5

The results represented above show the variation of compressive and tensile strength with the introduction of fibers. M1 & M3 mixtures have same properties except that M3 includes 0.13 steel fibers by weight of cement, which increases the compressive strength by 58.9% while the compressive strength is increased by 116% at 28 days. M2 & M4 mixtures have same properties except that M4 includes 0.22 steel fibers by weight of cement, which increases the compressive strength by 15.7% while the compressive strength is increased by 76.1% at 28 days.

Drop weight impact test [K. Habel, et al. 2008]

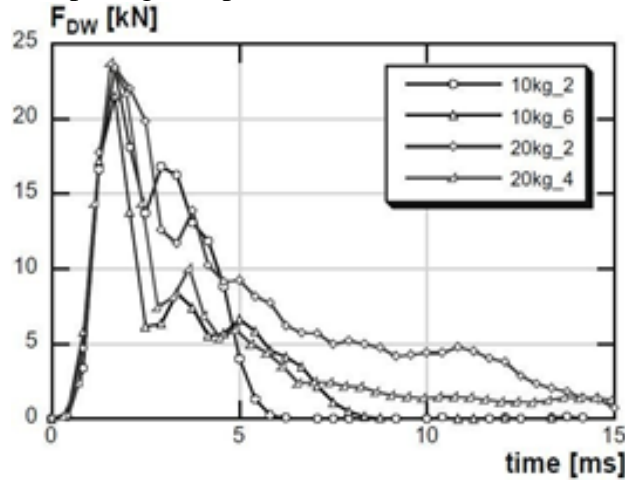


Fig 8a: Drop weight force v/s time

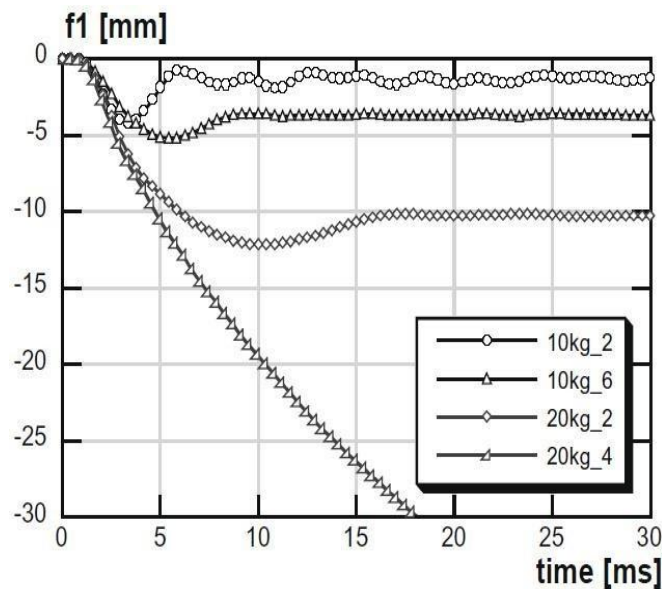


Fig 8b: Mid span deflection v/s time

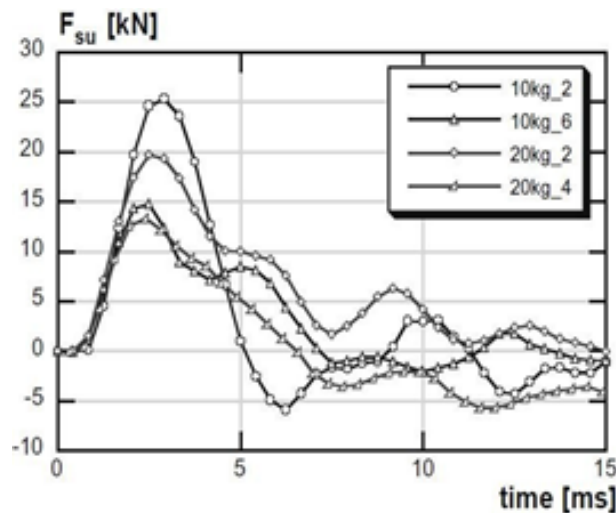


Fig 8c: Total support reaction v/s time

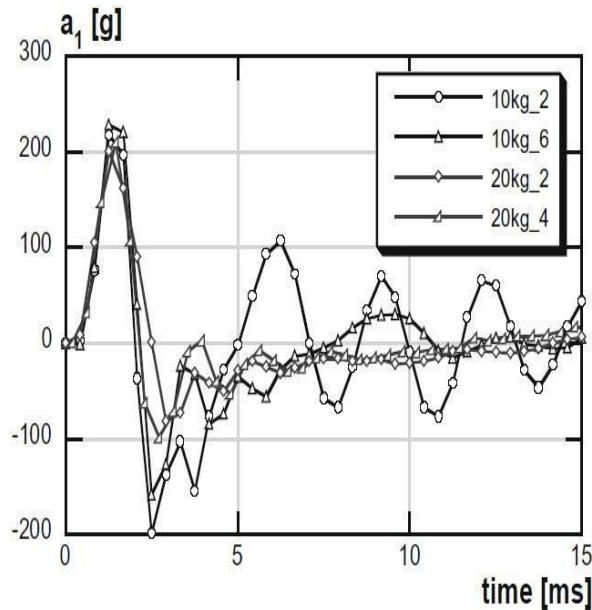


Fig 8d: Acceleration v/s time

The time histories for deflection, drop weight force, support reaction and strain arte are shown above in the figures during the first impact. Although the specimens are impacted with the drop weight until they fractured but out of 6 specimens tested with 20Kg weight fractured in single impact only, and hence various parameters could not be established for them. Some of the results are shown in the table given below in the table for the first impact.

The beams undergoing large deflection in first impact only fractured in less number of impacts while the less support reaction was observed in those specimens because of less inertial effect of the concrete specimen. However no direct correlation is observed between the total impact force and total support reactions due to the concrete in homogeneity and variable inertial forces on concrete specimen. The data obtained from strain gauge is a continuous series, and hence the maximum strain occurring in the concrete specimen can be selected from that data.

Specimen name (-)	Drop weight (kg)	Number of drops (-)	First drop			
			Max. fl (mm)	Max. $F_{DW}$ (kN)	Max. $F_{SR}$ (kN)	Max. $d_t/dt$ ( $s^{-1}$ )
10kg_1	10.3	4	-4.1	23.0	24.5	2.5
10kg_2	10.3	5	-4.2	23.4	25.3	2.6
10kg_3	10.3	5	-4.6	22.8	26.4	3.0
10kg_4	10.3	3	-5.1	23.5	18.5	2.4
10kg_5	10.3	3	-5.1	21.6	16.7	2.8
10kg_6	10.3	3	-5.2	21.5	14.8	1.9
10kg_7	10.3	3	-5.7	23.3	20.9	2.7
20kg_1	20.6	2	-6.5	26.3	30.7	2.3
20kg_2	20.6	2	-12.2	23.4	19.7	3.1
20kg_3	20.6	1	- <sup>a</sup>	23.0	14.3	3.5
20kg_4	20.6	1	- <sup>a</sup>	23.8	13.3	3.4
20kg_5	20.6	1	- <sup>a</sup>	23.8	17.1	3.3
20kg_6	20.6	1	- <sup>a</sup>	22.8	16.5	2.9

<sup>a</sup> Not applicable due to complete failure of the specimen at first drop.

Table 6 Results of drop weight impact test over UHPFRC (K. Habel, et al. 2008)

Drop weight impact test [H.S. Arel]

Table 7 Constituents of UHPFRC

Specimens	Components (kg/m <sup>3</sup> )										
	Cement	Quartz	Water	SF 1	SF 2	SF 3	L <sub>c</sub> 8 mm	L <sub>c</sub> 13 mm	L <sub>c</sub> 16 mm	SP	w/c
SF1-8 mm	640	1170	135	214	-	-	145	-	-	35	0.21
SF1-13 mm	640	1170	135	214	-	-	-	145	-	35	0.21
SF1-16 mm	640	1170	135	214	-	-	-	-	145	35	0.21
SF2-8 mm	640	1170	135	-	214	-	145	-	-	37.5	0.21
SF2-13 mm	640	1170	135	-	214	-	-	145	-	37.5	0.21
SF2-16 mm	640	1170	135	-	214	-	-	-	145	37.5	0.21
SF3-8 mm	640	1170	135	-	-	214	145	-	-	40	0.21
SF3-13 mm	640	1170	135	-	-	214	-	145	-	40	0.21
SF3-16 mm	640	1170	135	-	-	214	-	-	145	40	0.21

SF: silica fume, SP: superplasticizer, w/c: water/cement ratio, L<sub>c</sub>: length of steel fiber.

Table 8 Chemical composition of cement, SF and quartz

Components (%)	Cement	Quartz Sand	SF 1	SF 2	SF 3
SiO <sub>2</sub>	18.4	99.7	93.95	94.24	94.49
CaO	62.6	0.01	0.27	0.43	0.59
Al <sub>2</sub> O <sub>3</sub>	4.1	0.04	0.21	0.33	0.41
Fe <sub>2</sub> O <sub>3</sub>	3.08	0.05	0.71	0.95	0.54
MgO	2.4	0.01	0.25	0.88	1.03
K <sub>2</sub> O	0.7	-	1.27	0.64	0.49
SO <sub>3</sub>	2.6	-	0.26	0.3	0.34
Na <sub>2</sub> O	0.2	-	0.1	0.14	0.31
C <sub>3</sub> S	61.3	-	-	-	-
C <sub>2</sub> S	12	-	-	-	-
C <sub>3</sub> A	6.5	-	-	-	-
C <sub>4</sub> AF	7.3	-	-	-	-
Loss ignition	2.2	0.13	2.92	2.21	1.85
Specific surface area (m <sup>2</sup> /kg)	415	255	17,200	20,000	27,600
Specific gravity (g/cm <sup>3</sup> )	3.1	2.8	2.3	2.2	2.15
45 μm sieve residue	1.17	42.05	35.3	26.13	0.54

As can be seen that the high cement content in the constituents of UHPFRC makes it very costly. Therefore researches have been conducted to find the amount of pozzolanas to be added in the concrete mixture so as to achieve economy without much reduction in the strength of concrete. The above research introduces different kinds of silica fume with different kinds of steel fibers in the mixture. They utilized 1050 Kg/m<sup>3</sup> of cement in mix proportioning of UHPFRC while the author in this research has used only 640 Kg/m<sup>3</sup> of cement and 1170 Kg/m<sup>3</sup> of quartz and 214 Kg/m<sup>3</sup> of silica fume. Different shape and size of steel fibers are studied to check the effect of curing regime in UHPFRC.

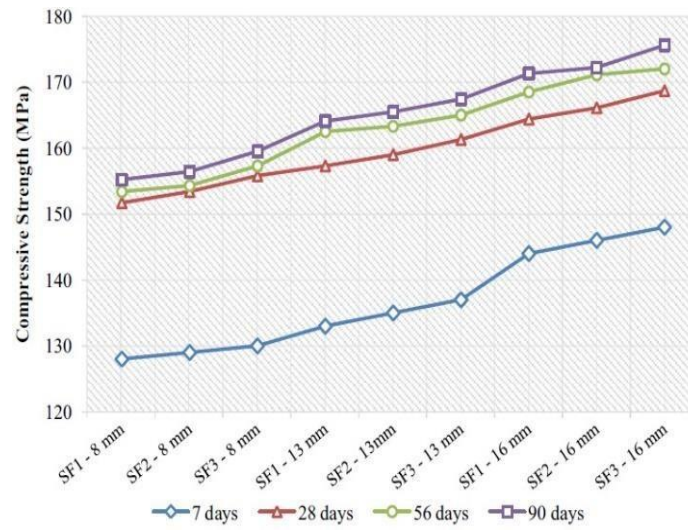


Fig 9a: Comp strength with standard curing

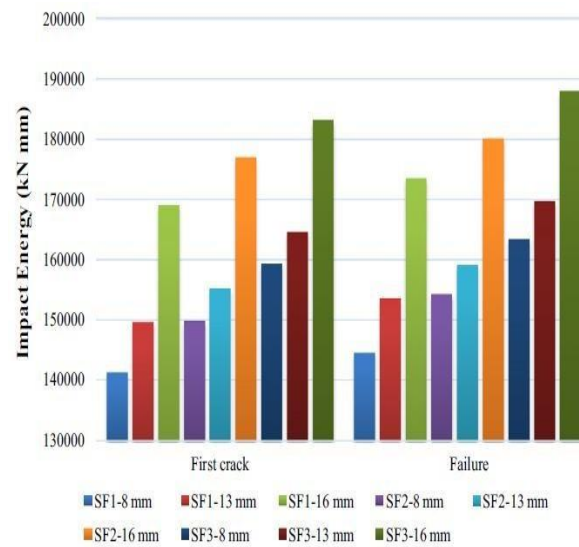


Fig: 9b Impact resistance after 90days of standard curing

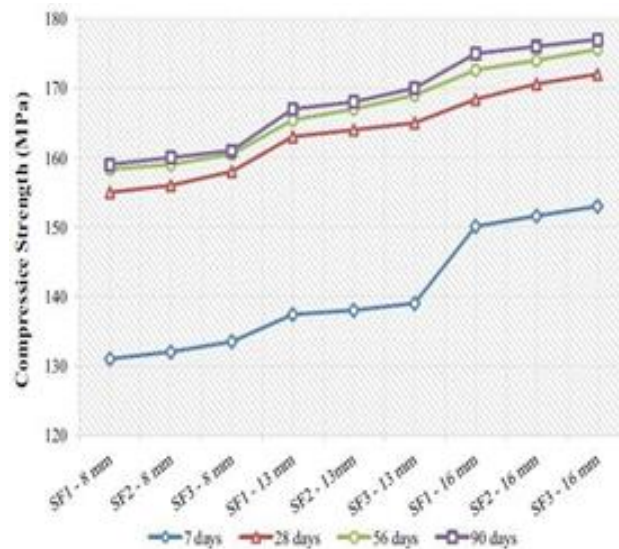


Fig 7 9c: Comp strength with steam curing

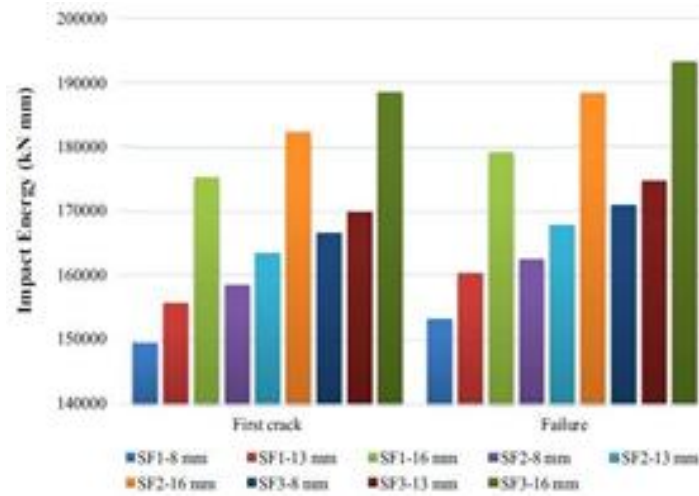


Fig 9d: Impact resistance after 90 days of steam curing

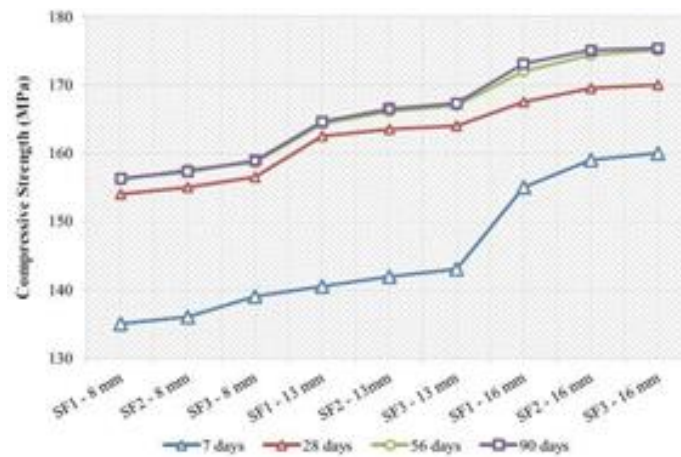


Fig 9e: Comp strength with hot water curing

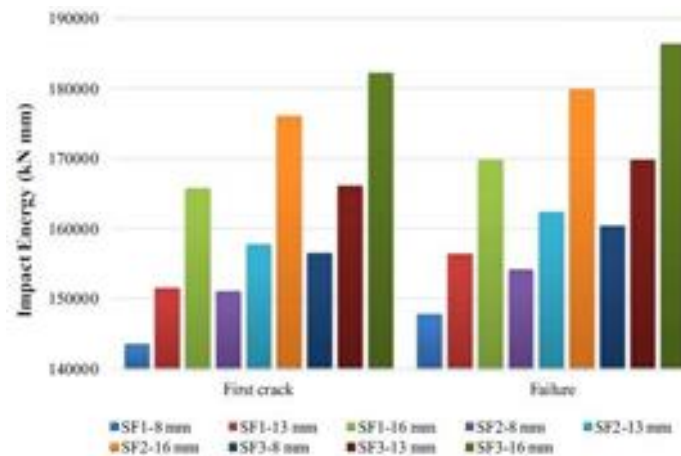


Fig 9f: Impact resistance after 90 days of hot water curing

From the histograms it can be observed that the compressive strength and impact energy increases with increase in fiber length. This is because the smaller length fibers are unable to develop enough pull out strength due to lesser length. Since the compressive strength of matrix phase is very high, therefore the fibers introduced should also be able to sustain high strength.

The constituent details of SF1, SF2 and SF3 are given in the table above. At standard curing condition, for the same silica fume type, the impact energies at failure are 16400, 17000 and 18800 KN-mm for 8mm, 13mm and 16mm steel fiber length for SF3. Also the impact energies at failure are 17300, 18000 and 18800 KN-mm for 16mm steel fiber length with SF1, SF2 and SF3 respectively.

Since the curing conditions improve the packing density of the mixture keeping other factors constant, therefore the compressive strengths and impact energy obtained for steam curing are higher than that of standard curing. But the curing with hot water increases the water at the surface of specimen which increases the porosity of the material therefore the compressive strength and impact energy obtained with hotwater curing are even less than that obtained with standard curing regime.

**PENDULUM IMPACT TEST [YU ET AL 2016.]**

The concrete specimen is freely kept over the equipment floor. The V-notch lever arm is raised to a height of about 3.2m and left to rotate freely over the rotations point. The rotating lever arm strikes with the concrete specimen. Since the specimen is kept freely over the surface therefore the specimen also attains a velocity along with the residual velocity remaining in the falling lever arm. The concrete specimen is again subjected to impact if not fractured in first time (Yu et al 2016).



Fig 10a Pendulum impact test equipment

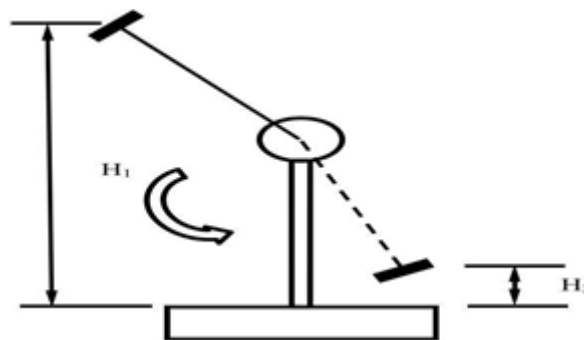


Figure 10b Schematic diagram of pendulum impact test

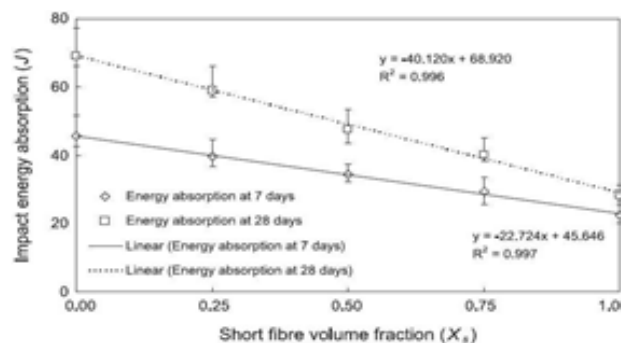


Fig 11 Impact energy v/s short straight fiber volume fractions (Yu et al 2016).



Table 9 Constituents of UHPFRC (Yu et al 2016).

No.	C (kg/m <sup>3</sup> )	LP (kg/m <sup>3</sup> )	M-S (kg/m <sup>3</sup> )	N-S (kg/m <sup>3</sup> )	ns (kg/m <sup>3</sup> )	W (kg/m <sup>3</sup> )	SP (kg/m <sup>3</sup> )	LSF (Vol. %)	SSF (Vol. %)	HF (V)
1	594.2	265.3	221.1	1061.2	24.8	176.9	44.2	0	0	0
2	594.2	265.3	221.1	1061.2	24.8	176.9	44.2	2.0	0	0
3	594.2	265.3	221.1	1061.2	24.8	176.9	44.2	1.5	0.5	0
4	594.2	265.3	221.1	1061.2	24.8	176.9	44.2	1.0	1.0	0
5	594.2	265.3	221.1	1061.2	24.8	176.9	44.2	0.5	1.5	0
6	594.2	265.3	221.1	1061.2	24.8	176.9	44.2	0	2.0	0
7	594.2	265.3	221.1	1061.2	24.8	176.9	44.2	0	0	2
8	594.2	265.3	221.1	1061.2	24.8	176.9	44.2	0.125	0.375	1.5
9	594.2	265.3	221.1	1061.2	24.8	176.9	44.2	0.5	0	1.5
10	594.2	265.3	221.1	1061.2	24.8	176.9	44.2	0	0.5	1.5

C: cement, LP: limestone powder, M-S: microsand, N-S: normal sand, ns: nano-silica, W: water, SP: superplasticizer, LSF: long straight fibre, SSF: short straight fibre, HF: hooked fibre.

The introduction of fibers increase the post peak strength of concrete but the short length fibers or the low aspect ratio fibers are unable to develop enough pull out strength before they fracture. The same can be observed from the above given graph. The impact energy absorption capacity reduces with the increase in short fiber content because the short aspect ratio fibers are subjected to fracture before the development of shear bond strength. For all the above cases the total fiber fraction is kept constant and only the content of short fibers is varied.

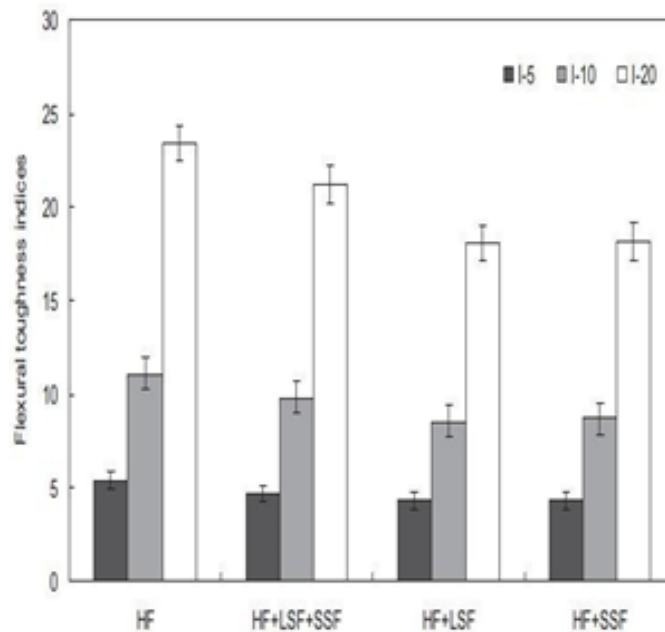


Fig 12 Flexural toughness indices of UHPFRC based on ASTM C1018-97 (Spiesz, and Brouwers, 2015)

The flexural toughness index also follows the same trend. It also reduces with increase in short fiber content keeping the total fiber content constant. The toughness index is the ratio of deflection at specified deflection w.r.t. the deflection at first crack. Some of the toughness indices can be observed in the above histogram.

Drop weight impact test over concrete (Wu et al. 2015)

Table 10 Different loading case for drop weight impact test (Wu et al. 2015)

Top material	Cases	Hammer weight, m/kg	Drop height, H/m	Max impact force, $P_{max}$ /kN	Ultimate tensile strain, $\epsilon_{ij}$
Aluminum	Different drop heights with a constant weight	4	0.5	45.3	202
		4	1.0	56.8	194
		4	1.5	67.4	186
		4	2.0	71.5	225
	Different weights with a constant drop height	1	2.0	42.1	198
		2	2.0	61.1	245
		3	2.0	65.0	229
		4	2.0	71.5	225
Rubber	Different drop heights with a constant weight	4	0.5	17.7	202
		4	1.0	28.9	231
		4	1.5	35.0	193
		4	2.0	43.2	245

The author used different kinds of alloy pads to save the force transducer from damage while the impact of falling hammer mass over the concrete specimen. The drop weight and drop height are also varied to check their effects. The potential energy increases with increase in either mass of hammer or the dropping height of hammer, and hence the fracture energy absorbed by the specimen also increases.

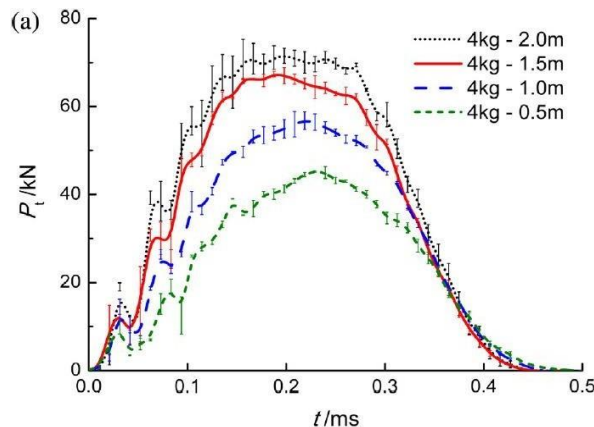


Fig 13a Time history of total imparted force

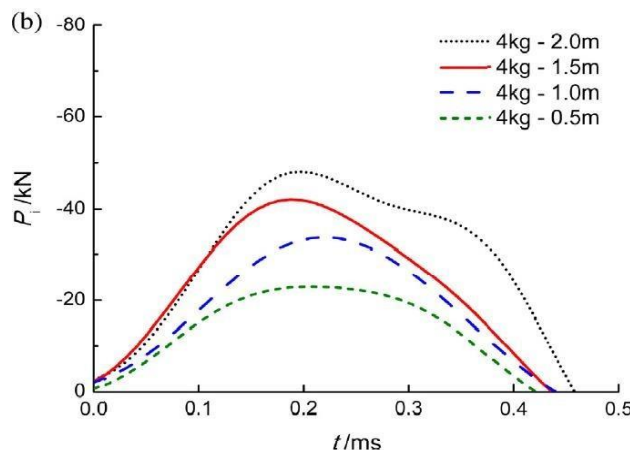


Fig 13b Time history of inertial force

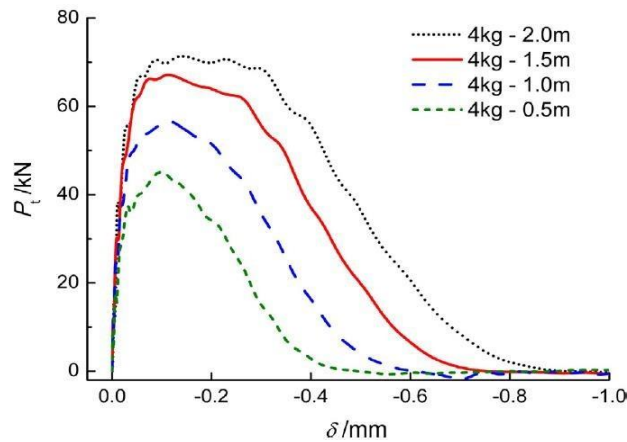


Fig 13c Total force v/s deflection curve

The time histories are given for the total force, inertial force and deflection of the concrete beam. In the case under consideration, the hammer mass is kept constant and the drop height is varied. It can be observed that the potential energy of hammer mass increases with increase in height and hence the total force imparted by the hammer also increase. From the time histories given above it can be observed that keeping the mass constant and changing the drop height, the concrete specimen returns to its original position within same time frame in all cases. It is attributed to the striking velocity of hammer because increasing the kinetic component of concrete specimen deflection will change the rate of deflection.

The inertial forces also increase with increase in momentum of falling hammer mass. The inertial forces can be determined through the equation. The deflection varies with the variation in drop height but there is direct correlation seen between the two.

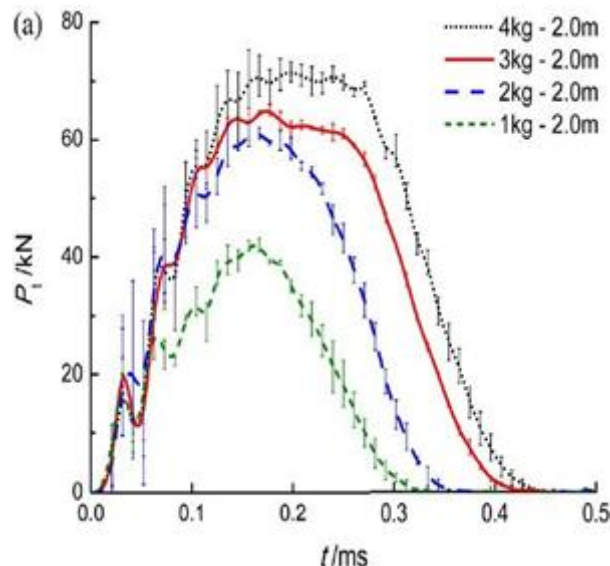


Fig 14a Time history of total imparted force

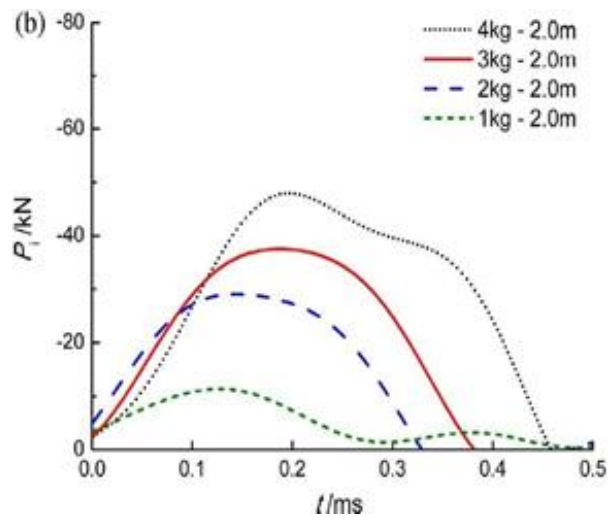


Fig 14b Time history of inertial force

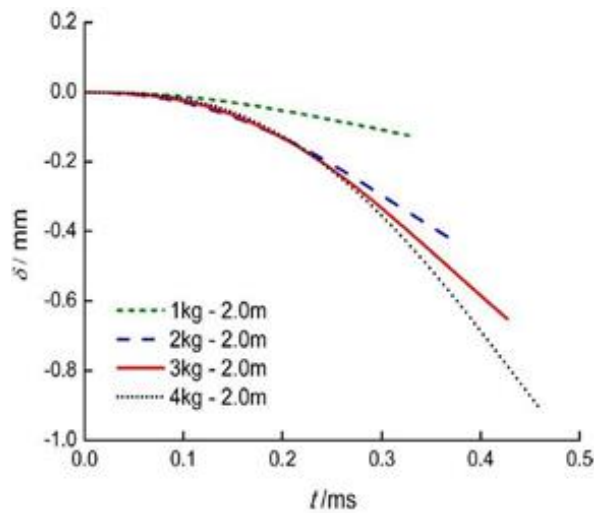


Fig 14c Time history of deflection curve

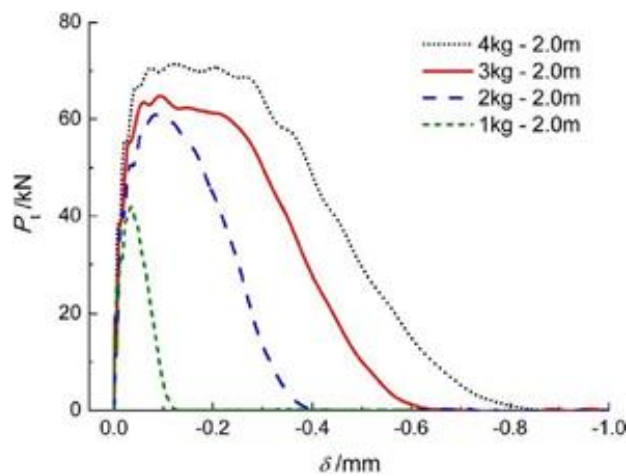


Fig 14d Total force v/s deflection curve

Table 11 Results for above tests [33]

Top material	Hammer weight, m/kg	Drop height, H/m	Force rate, $\dot{P}$ (MN/s)	CIF	Strain rate, $\dot{\epsilon}$ (s <sup>-1</sup> )	DIF	$W_d$
Aluminum	4	0.5	219	4.72	2.0	2.34	5.6
	4	1.0	403	5.92	2.5	2.79	6.4
	4	1.5	429	7.02	2.3	3.00	10.0
	4	2.0	494	7.45	3.2	3.03	10.0
	1	2.0	238	4.38	1.7	3.33	2.1
	2	2.0	405	6.37	2.3	3.38	6.8
	3	2.0	469	6.77	2.3	2.92	10.4
	4	2.0	494	7.45	3.2	3.03	10.0
Rubber	4	0.5	36	1.84	0.3	1.68	4.7
	4	1.0	68	3.01	0.7	2.25	8.4
	4	1.5	90	3.64	1	2.05	10.6
	4	2.0	126	4.50	1.8	2.33	12.3

The time histories are given for the total force, inertial force and deflection of the concrete beam. In the case under consideration, the drop height is kept constant and hammer mass is varied. It can be observed that increase in hammer mass also increase the potential energy and striking velocity of hammer. In introduces the force rate effects. There is no direct correlation observed between the total hammer mass and the deflection of concrete specimen. According to newton’s law, the force is given by rate of change of momentum. In all the above given cases, the momentum increases with increase in mass and velocity both but in the drop weight test, it is primarily governed by hammer mass. Therefore the strain rate effects are primarily observed in case of change in hammer mass keeping the drop height constant.

Some results obtained from the experiments are given below for different drop weight, different drop height and change in the alloy pad too. It is evident from the above graph that the dynamic load carrying capacity of concrete specimen is always higher than its quasi static strength. The maximum dynamic load carrying capacity again increases with increase in force rate. The force rate can either be increased by increasing the falling hammer mass or it can also be increased by increasing the drop height. In both the cases the potential energy of the hammer mass will increase which will increase the force rate, and hence the DIF and CIF increase (Wu et al. 2014, Ulzurrun and Zanuy 2017).

Ideally the DIF & CIF increase with increase in strain rate or increase in force rate. This is attributed to the inertial forces coming in to the picture. CIF is always higher because it includes the total force while DIF includes only the deforming force. Although the falling graph obtained in case of constant drop height and different drop weights may be due to the in homogeneity of concrete.

**V. CONCLUSION**

- UHPFRC is sustainable material for future infrastructure development because of its High strength parameter and crack arresting mechanism which help in fulfilling ‘limit state of serviceability’ criteria.
- Pozzolanas (Slag, fly ash and silica fume) improve the strength properties of FRC, but suitability must be checked for different kinds of fiber and w/b ratio.
- Pozzolanic materials reduce the autogenous shrinkage of FRC up to 30% but the effect of metakaolin also depend over w/b ratio. Metakaolin reduced shrinkage significantly with w/b ratio 0.28 but no significant effect observed with w/b ratio equal to 0.35.
- The dynamic stress or Strain Capacity of UHPFRC also depend over the specimen dimensions due to inertial effects coming in to picture during sudden momentum change.

- None of the impact test can be standardized because of the different principles attributed in all the impact type tests.

## REFERENCES

1. M. Wu, C. Zhang, and Z. Chen, "Determining the impact behavior of concrete beams through experimental testing and meso-scale simulation: II. Particle element simulation and comparison," *Eng. Fract. Mech.*, vol. 135, pp. 113-125, 2015, doi:10.1016/j.engfracmech.2014.12.020.
2. K. Habel and P. Gauvreau, "Response of ultra-high performance fiber reinforced concrete (UHPFRC) to impact and static loading," *Cem. Concr. Compos.*, vol. 30, no. 10, pp. 938–946, 2008, doi:10.1016/j.cemconcomp.2008.09.001.
3. M. Wu, Z. Chen, and C. Zhang, "Determining the impact behavior of concrete beam through experimental testing and meso-scale simulation: I. Drop-weight tests," *Eng. Fract. Mech.*, vol. 135, pp. 941-12, 2015, doi:10.1016/j.engfracmech.2014.12.019.
4. P. Rossi, "Cement & Concrete Composites Influence of fibre geometry and matrix maturity on the mechanical performance of ultra high-performance cement-based composites," *Cem. Concr. Compos.*, vol. 37, pp. 246–248, 2013, doi: 10.1016/j.cemconcomp.2012.08.005.
5. S. El-dieb, "Mechanical, durability and microstructural characteristics of ultra-high-strength self-compacting concrete incorporating steel fibers," *Mater. Des.*, vol. 30, no. 10, pp. 4286–4292, 2009, doi:10.1016/j.matdes.2009.04.024.
6. A.M.T. Hassan, S.W. Jones, and G.H. Mahmud, "Experimental test method to determine the uniaxial tensile and compressive behavior of ultra high performance fibre reinforced concrete (UHPFRC)," *Constr. Build. Mater.*, vol. 37, pp. 874–882, 2012, doi:10.1016/j.conbuildmat.2012.04.030.
7. R. Yu, P. Spiesz, and H. J. H. Brouwers, "Mix design and properties assessment of Ultra-High Performance Fibre Reinforced Concrete (UHPFRC)," *Cem. Concr. Res.*, vol. 56, pp. 29–39, 2014, doi:10.1016/j.cemconres.2013.11.002.
8. Ulzurrun and C. Zanuy, "Flexural response of SFRC under impact loading," *Constr. Build. Mater.*, vol. 134, pp. 397–411, 2017, doi:10.1016/j.conbuildmat.2016.12.138.
9. M. Popa, O. Corbu, Z. Kiss, and R. Zagon, "Achieving Mixtures of Ultra-High," *Construcții*, no. 1, 2013.
10. ASTM, "Standard Test Method for Compressive Strength of Hydraulic Cement Mortars (Using 2-in. or [50-mm] Cube Specimens) 1," *Chem. Anal.*, vol. 04, no. C109/C109M – 11b, pp. 1–9, 2010, doi:10.1520/C0109.
11. ASTM C880, "Standard Test Method for Flexural Strength of Dimension Stone," *Annu. B. ASTM Stand.*, vol. 03, pp. 98–100, 1999, doi:10.1520/C0880.
12. ASTM C157, "Standard Test Method for Length Change of Hardened Hydraulic-Cement Mortar and," *Annu. B. ASTM Stand.*, vol. 08, no. c, pp. 1–7, 2016, doi: 10.1520/C0157.